ELSEVIER

Journal of Nuclear Materials 307–311 (2002) 696–700

journal of nuclear materials

www.elsevier.com/locate/jnucmat

Structure–mechanics relationships in proton irradiated pure titanium

T. Leguey *, N. Baluc, R. Schäublin, M. Victoria

CRPP-EPFL Fusion Technology Materials, 5232 Villigen-PSI, Switzerland

Abstract

Radiation effects on the mechanical behavior and the microstructure of pure hcp titanium polycrystals have been investigated. Results have been analyzed in the frame of a dispersed obstacle hardening model and compared to those previously obtained for pure metals with a fcc or bcc structure, such as Cu and Pd or Fe, respectively. Differences in the defect accumulation rate and the dose dependence of hardening are discussed in terms of possible irradiation hardening mechanisms for the hcp structure.

1. Introduction

During the past 10 years, a number of investigations of radiation damage effects have been performed on pure fcc and bcc metals, showing significant differences in the defect accumulation rate and the dose dependence of hardening between these two structures [1]. In hcp metals, however, these aspects remain still unclear. The anisotropy of the hexagonal lattice complicates the problem in two respects; (i) defect migration becomes anisotropic which can lead to different damage accumulation behavior, and (ii) distinct types of dislocations exist, moving and reacting with the defects in a different way [2]. The changes in microstructure and mechanical properties after irradiation of many hcp pure metals and alloys have been object of numerous studies, see for instance [3–7], and progress in the understanding of radiation damage effects in these materials is continuing [8–10].

The present paper is aimed at describing the effects of radiation on the mechanical behavior and microstructure of pure Ti polycrystals, which have been investigated by combining conventional mechanical testing with transmission electron microscopy (TEM) observations. Results are tentatively compared with those previously obtained for pure metals with an fcc or bcc structure.

2. Experimental procedures

Flat tensile specimens of 8 mm gauge length and 2.5 mm width were prepared from polycrystalline cold-rolled (0.5 mm thick) foils of pure titanium (99.999%). The tensile axis was chosen parallel to the rolling direction. The specimens were mechanically polished to a thickness of about 300 μm. They were then annealed in vacuum at 973 K for 5 h. The final grain size was about 80 μm.

A series of specimens were irradiated in the proton irradiation experiment facility, at the Paul Scherrer Institute, with 590 MeV protons. These irradiations were performed at two different temperatures, 300 and 523 K, to doses ranging between 4×10^{-4} and 4×10^{-1} dpa. The damage rate was approximately 10^{-7} dpa s^{-1}.

The as-annealed and irradiated specimens were deformed at the irradiation temperature using a computer-controlled Zwick testing machine. Experiments at 523 K were performed in argon atmosphere. The strain rate was 4×10^{-5} s^{-1}. Deformation experiments were performed up to fracture.

* Corresponding author. Permanent address: Depto. de Física, Univ. Carlos III de Madrid, 28911 Leganés, Spain. Tel.: +34-91 6249413; fax: +34-91 6248749.

E-mail address: leguey@fis.uc3m.es (T. Leguey).

0022-3115/02/$ - see front matter
PII: S0022-3115(02)01190-X

The defects produced by deformation and/or irradiation were imaged in a JEOL 2010 transmission electron microscope operating at 200 kV, using the bright/dark field and weak beam techniques. The best diffraction conditions to analyze dislocations were found to be close to the zone axis $[2\bar{1}\bar{1}0]$. There, the diffraction vectors (0002), $(01\bar{1}0)$ and $(01\bar{1}1)$ allowed to identify the Burgers vectors *a* and *c*. The best diffraction vector in terms of image quality is $(01\bar{1}1)$.

Specimens for TEM were sectioned from the as-annealed, irradiated and/or deformed specimens by using an electrical discharge machine. They were electrochemically thinned at −35 °C, by means of a standard double jet technique, in a solution of ethanol containing 3 vol.% perchloric acid and 37 vol.% 2-butoxyethanol. The applied voltage was 20 V.

The accumulated dose of the irradiated samples was calculated for each TEM specimen from the activity measured with a gamma spectrometer.

3. Results and discussion

3.1. Defect microstructure

Specimens irradiated at room temperature to 4×10^{-4}, 4×10^{-3} and 3×10^{-2} dpa were investigated by TEM prior to deformation. Fig. 1(a) shows an unirradiated sample. Fig. 1(b) shows a typical TEM micrograph of samples irradiated up to 4×10^{-3} dpa. Some defect clusters can be observed in dislocation free areas. Note that the background intensity can be misleading as illustrated in the previous image. Fig. 1(c) shows a typical TEM micrograph obtained for specimens irradiated to 3×10^{-2} dpa, which reveals black dot damage resulting from the irradiation. They were identified as loops that form nearly planar groups lying in the basal plane. Their character (vacancy or interstitial) and Burgers vector have not yet been determined. These groups appear homogeneously distributed in all the grains.

The samples irradiated to 4×10^{-4} dpa exhibit the same microstructure characteristics, but with a lower defect cluster density. The defect size distribution was determined in all irradiated specimens and it appears that defects have a mean size of 2.4 nm over a range of doses. About 5% of them are identified as dislocation loops with apparent sizes up to 10 nm.

A high density of dislocations is present at 4×10^{-3} dpa, in some regions. Some of them were seen to be highly mobile under the electron beam, leaving slip traces at the surfaces. Tilt experiments confirmed their basal character. While they also appear in specimens irradiated to the lowest dose, 4×10^{-4} dpa, they are not visible in unirradiated specimens or in the specimens irradiated up to 3×10^{-2} dpa. This high mobility is an indication that the defects created during the irradiation are not strong enough to pin the dislocations and/or the irradiation-induced dislocation loops.

Fig. 2 shows the defect density (*N*) as a function of the accumulated dose for all the observed samples irradiated at 300 K. A linear fit of the data gives a slope of 0.55, significatively lower than the values obtained for

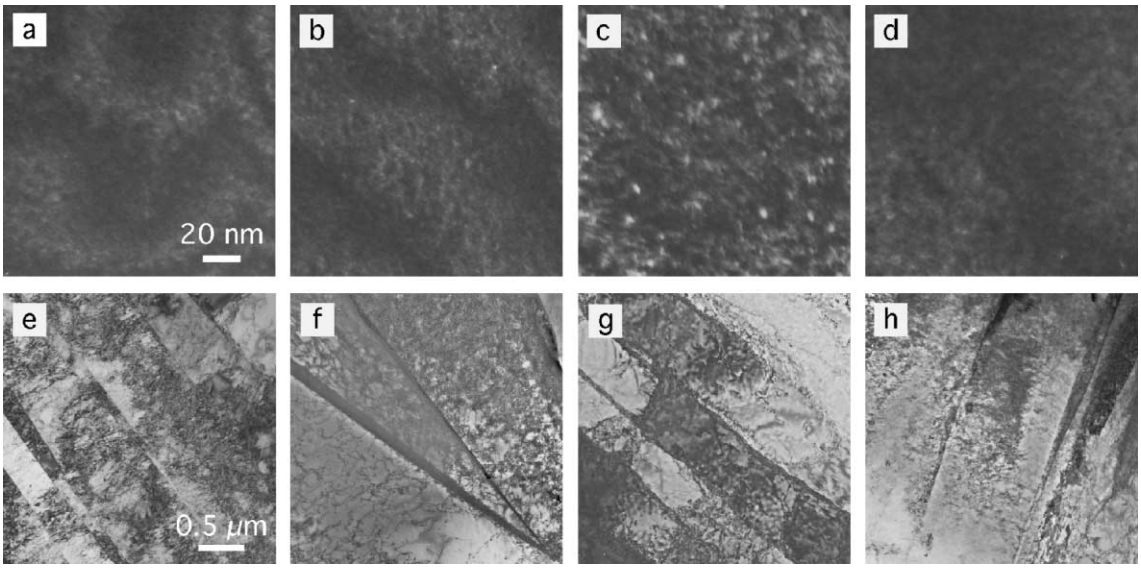

Fig. 1. TEM images of pure Ti: (a) unirradiated, (b) irradiated at 4×10^{-3} dpa, (c) irradiated at 3×10^{-2} dpa, (d) irradiated at 4×10^{-1} dpa and deformed, (e) unirradiated and deformed, (f) irradiated at 4×10^{-3} dpa and deformed, (g) irradiated at 3×10^{-2} dpa and deformed, (h) irradiated at 4×10^{-1} dpa and deformed. Both irradiation and deformation temperature was 300 K.

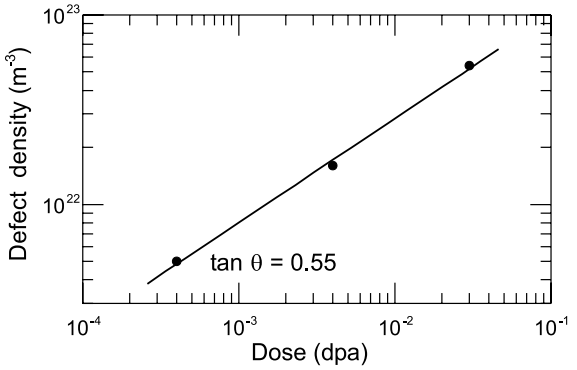

Fig. 2. Defect cluster density versus irradiation dose at room temperature.

Cu, $\tan\theta = 1$ [11], Pd, $\tan\theta = 0.9$ [12] and Fe, $\tan\theta = 0.96$ [13]. These materials present a clear linear dependence of the defect accumulation rate in a first stage followed by a $(\text{dose})^{1/2}$ dependence related to saturation. In the case of Ti no clear linear stage is observed, at least for the investigated dose range. TEM investigation of the samples irradiated at 523 K is under way and will be reported later.

3.2. Mechanical behavior

Fig. 3 illustrates tensile stress–strain curves of the annealed and irradiated specimens. Fig. 3(a) shows results from tensile tests carried out at room temperature on samples irradiated at 300 K, while Fig. 3(b) shows results from tests performed at 523 K on samples irradiated at the same temperature. No yield drop was observed at any irradiation dose or temperature. Main effects of irradiation can be described as radiation hardening and reduction of ductility.

Samples irradiated at 300 K, however, do not exhibit a clear loss of ductility with increasing dose up to 4×10^{-1} dpa, due to the large scattering in the values obtained for total elongation. The reason for this dispersion could be that the thickness of the specimens is small compared to the grain size. Therefore, only a few grains in the thickness are actually contributing to the deformation process. Nonetheless, the samples irradiated at 523 K exhibit a clear reduction in ductility with increasing dose. The total elongation measured for the samples irradiated and tested at 523 K decreases by about 10% when the damage level reaches 9×10^{-2} dpa.

The radiation hardening, given by the increase in the yield stress ($\Delta\sigma_y$) as a function of dose, is plotted in Fig. 4 for both sets of specimens. The values obtained at room temperature follow a linear behavior (on a log–log scale), for all the investigated doses. No saturation is observed in this range. The calculated slope of the linear fit is 0.23, that is, $\Delta\sigma_y$ is proportional to the fourth root

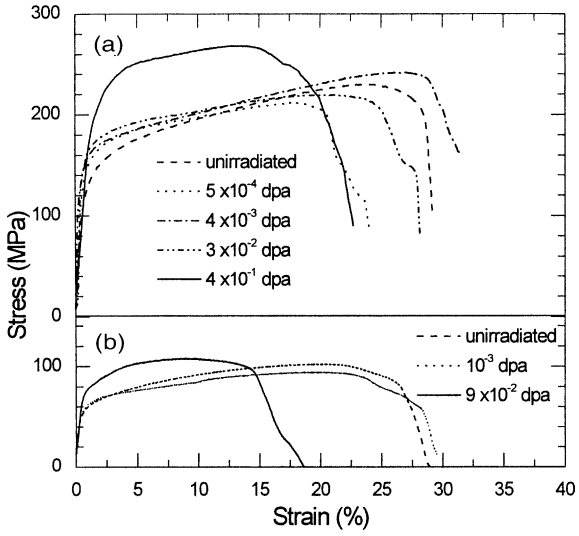

Fig. 3. Tensile stress–strain curves of pure Ti irradiated and tested at (a) room temperature, (b) 523 K.

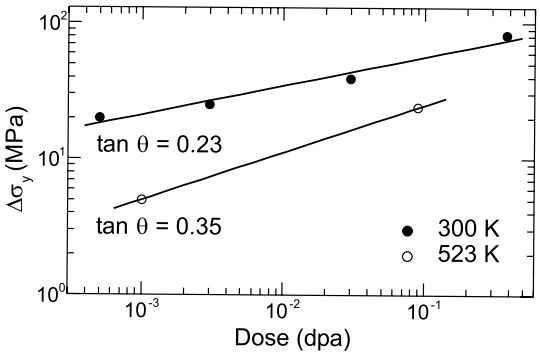

Fig. 4. Increase in yield stress versus irradiation dose at room temperature and at 523 K.

of the dose. Results from the specimens irradiated at 523 K show a lower increase in the absolute value of the yield stress, but the calculated slope increases to 0.35, that is $\Delta\sigma_y$ is proportional to the third root of the dose.

The results obtained at room temperature can be compared with those obtained for other proton-irradiated pure metals. The behavior of $\Delta\sigma_y$ for Ti irradiated at room temperature is closer to that of polycrystalline bcc Fe ($\Delta\sigma_y$ proportional to the fifth root of the dose [13]), than to Pd and Cu single crystals. In the latter cases, $\Delta\sigma_y$ was found to be proportional to the third root [12] and to the square root [11] of the dose, respectively. Both Ti and Fe exhibit lower increase rates, however, the absolute values of $\Delta\sigma_y$ are much lower in the case of Ti than in Fe, showing that radiation damage at the investigated doses in titanium has a less effect. The values of $\Delta\sigma_y$ at 523 K are also lower for Ti than for Fe [13], but while results at 523 K for Fe show no

dependence of $\Delta\sigma_y$ on dose, the dependence obtained for Ti at that temperature becomes obvious (see Fig. 4).

TEM micrographs of unirradiated samples and samples irradiated at room temperature to doses of 4×10^{-3}, 3×10^{-2} and 4×10^{-1} dpa and subsequently deformed at the same temperature are shown in Fig. 1(d)–(h). After the earliest stages of the deformation process, the defect clusters are not visible anymore, apart from a few isolated dislocation loops, even for the highest dose (Fig. 1(d)). Arrays of parallel twins and deformation cells are present. Dislocation walls formed in the first-order prismatic planes by the slip of *a*-type dislocations. No differences were found between the irradiated (Fig. 1(f)–(h)) and the unirradiated specimens (Fig. 1(e)).

3.3. Radiation hardening

The dose dependence of the yield stress increment, $\Delta\sigma_y$, and the defect density (N) have been found to be proportional to 0.23 and 0.55, respectively, which leads to a relationship $\Delta\sigma_y \propto N^{0.42}$. The same exponent was found for Pd [12], while a value of 0.5 was found for Cu [11]. Such a square root dependence is consistent with the idea of a disperse obstacle hardening model with dislocation loops acting as hardening sources [14]. In such a model, the radiation hardening can be written as

$$\Delta\tau = \alpha\mu b\sqrt{d \cdot N}, \tag{1}$$

where $\Delta\tau$ is the change in critical resolved shear stress due to irradiation, μ is the shear modulus (42 GPa for Ti), b the magnitude of the Burgers vector (0.295 nm for *a*-type dislocations in Ti), d is the defect mean size (2.4 nm), N the defect density and α a constant related to the strength of the obstacle [14]. Eq. (1) should be multiplied by the Taylor's factor ($M = 5$ for titanium polycrystals [15]) to convert to tensile stresses.

Fig. 5 shows $\Delta\sigma_y$ as a function of $(d \cdot N)^{1/2}$. As it can be seen, the extrapolation of the linear fit to lower densities yields $\Delta\sigma_y(0) \neq 0$, which is inconsistent with the model. The same result is systematically found when the hardening model is applied to polycrystals [16–18]. A radiation-modified Hall–Petch effect has been proposed to explain the differences observed [16]. In any case, the corrections of the hardening model for polycrystals should be validated experimentally at low densities of defects. In this sense we are limited by the lowest density of defects resolvable in TEM measurements ($\simeq 10^{21}$ m^{-3}). However, from the data plotted in Fig. 5 and the slope of the linear fit, it was possible to calculate the strength of the obstacle, $\alpha = 0.04$. This value is considerably lower than that obtained for fcc metals, $\alpha = 0.1$ [11,12]. The corresponding breaking angle of the defects for Ti is calculated to be $\varphi_0 = 2 \cdot \cos^{-1}(\alpha/0.9)^{2/3}$ [19]. The obtained result is $\varphi_0 = 166°$, which corresponds to very weak obstacles, to be compared to the value of 154° obtained for Cu [11].

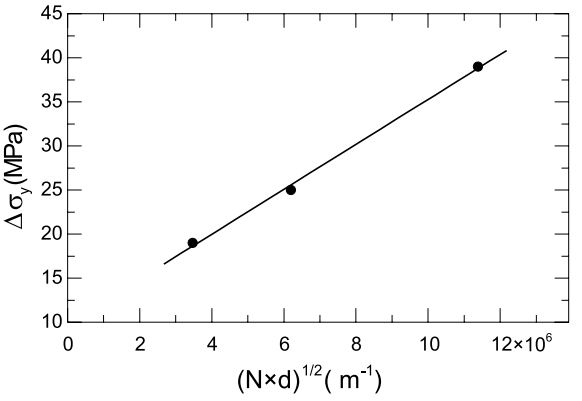

Fig. 5. Increase in yield stress versus $(d \cdot N)^{1/2}$ at room temperature, where d is the mean defect size and N is the defect density.

This preliminary study shows that Ti exhibits a different mechanical response to irradiation than that observed in other pure metals. It should be noted that the hardening model used here applies to the case of an isotropic source hardening, which is not the case of the defect morphology that develops in a hexagonal structure. To take in account this effect, the disperse obstacle hardening model as described above should be reformulated in terms of different interbarrier spacings. As a consequence, further investigations are needed in order to elucidate the type of defect clusters that are created by irradiation, in terms of Burgers vector, habit plane and interstitial/vacancy character.

4. Conclusion

Irradiation effects on the mechanical behavior and microstructure of pure Ti polycrystal have been investigated. As previously observed for fcc and bcc pure metals, proton irradiation at ambient temperature of pure hcp titanium produces hardening of the material, that was found to be proportional to the fourth root of the irradiation dose, a behavior similar to that of pure bcc iron. A stronger dependence is found at 523 K.

The microstructure of irradiated and/or deformed specimens is similar to that previously observed for pure fcc metals, the formation of twins being intrinsic to deformation of hcp titanium. When analyzed in the frame of a dispersed obstacles hardening model, the irradiation defects can be considered as weak obstacles, with a lower strength than those observed for pure fcc metals.

Acknowledgements

The present work has been supported by the European Fusion Technology Programme. The authors are

thankful to the Paul Scherrer Institute for providing access to its facilities.

References

[1] M. Victoria, N. Baluc, C. Bailat, Y. Dai, M.I. Luppo, R. Schäublin, B.N. Singh, J. Nucl. Mater. 276 (2000) 114.
[2] C.H. Woo, J. Nucl. Mater. 276 (2000) 90.
[3] A.L. Bement, in: Radiation Effects, Gordon and Breach Science, New York, USA, 1967, p. 671.
[4] J.E. Harbottle, Philos. Mag. A 38 (1) (1978) 49.
[5] M. Griffiths, J. Nucl. Mater. 205 (1993) 380.
[6] F.A. Garner, M.B. Toloczko, L.R. Geenwood, C.R. Eiholzer, M.M. Paxton, R.J. Puigh, J. Nucl. Mater. 283–287 (2000) 380.
[7] P. Marmy, T. Leguey, J. Nucl. Mater. 296 (2001) 155.
[8] D.J. Bacon, J. Nucl. Mater. 206 (2–3) (1993) 249.
[9] T. Díaz de la Rubia, H.M. Zbib, T.A. Khraisi, B.D. Wirth, M. Victoria, M.J. Caturla, Nature 406 (2000) 871.
[10] C.H. Woo, C.B. Soo, Philos. Mag. A 80 (6) (2000) 1299.
[11] Y. Dai, M. Victoria, in: I.M. Robertson et al. (Eds.), Proceedings of the MRS Symposium on 'Microstructure evolution during irradiation', Pittsburg, 1997, p. 319.
[12] N. Baluc, Y. Dai, M. Victoria, in: J.B. Bilde-Sørensen et al. (Eds.), Proceedings of the 20th Risø International Symposium on Materials Science on 'Deformation-Induced Microstructures: Analysis and Relation to Properties', Roskilde, Denmark, 1999, p. 245.
[13] M.I. Luppo, C. Bailat, R. Schäublin, M. Victoria, J. Nucl. Mater. 283–287 (2000) 483.
[14] A.L. Bement Jr., in: Proceedings of the 2nd International Conference on Strength of Metals and Alloys, ASM, Metals Park, OH, 1970, p. 693.
[15] T. Tanaka, H. Conrad, Acta Crystallogr. A 28 (1972) S165.
[16] S. Kojima, S.J. Zinkle, H.L. Heinisch, J. Nucl. Mater. 179–181 (1991) 982.
[17] M.L. Grossbeck, P.-J. Maziazs, A.F. Rowcliffe, J. Nucl. Mater. 191–194 (1992) 808.
[18] T. Muroga et al., J. Nucl. Mater. 225 (1995) 137.
[19] B. Reppich, in: R.W. Cahn, P. Haasen, E.J. Kramer (Eds.), Materials Science and Technology, vol. 6, 1994, p. 311.